Sustainable Chemistry

How to cite: *Angew. Chem. Int. Ed.* **2023**, *62*, e202217652
International Edition: doi.org/10.1002/anie.202217652
German Edition: doi.org/10.1002/ange.202217652

pH-Triggered Recovery of Organic Polymer Photocatalytic Particles for the Production of High Value Compounds and Enhanced Recyclability

*Rong Li, Julian Heuer, Thomas Kuckhoff, Katharina Landfester, and Calum T. J. Ferguson**

Abstract: Pseudo-homogeneous polymeric photocatalysts are an emerging class of highly efficient and tunable photocatalytic materials, where the photocatalytic centers are easily accessible. The creation of highly efficient photocatalytic materials that can be rapidly separated and recovered is one of the critical challenges in photocatalytic chemistry. Here, we describe pH-responsive photocatalytic nanoparticles that are active and well-dispersed under acidic conditions but aggregate instantly upon elevation of pH, enabling easy recovery. These responsive photocatalytic polymers can be used in various photocatalytic transformations, including Cr^{VI} reduction and photoredox alkylation of indole derivative. Notably, the cationic nature of the photocatalyst accelerates reaction rate of an anionic substrate compared to uncharged species. These photocatalytic particles could be readily recycled allowing multiple successive photocatalytic reactions with no clear loss in activity.

The emergence of visible light photocatalysts has facilitated the conversion of abundant solar energy to high value chemicals or electrical energy. To date, photocatalytic systems have been employed for a great number of applications, including aqueous pollutant degradation,[1–4] photodynamic therapy,[5–8] hydrogen evolution,[9–12] and organic transformations.[13–17] In particular, the wide scope of photocatalytic reactions (e.g. C–C coupling reactions,[18] C=C bond cleavage,[19] trifluoromethylation of arenes,[20] heterocycle formation,[21] and enantioselective alpha-alkylation[22]) is of great importance for organic chemistry to overcome the activation energy associated with a particular reaction under mild reaction conditions. Many investigations are undertaken with molecular homogeneous photocatalysts, including precious transition metal based photocatalysts[23] and organic photoredox catalysts,[24] which have been regarded as tunable alternatives to inorganic photocatalysts but at the expense of stability.[25–27]

The merger of molecular photocatalysts and heterogeneous polymers has realized efficient photocatalysis with enhanced stability compared to their molecular form. However, the difficulty in mass transport (e.g. substrates and oxygen) towards photocatalytic centers and maintaining stable dispersion of the photocatalytic materials can limit the performance of some heterogeneous polymeric photocatalysts.[28,29] Therefore, pseudo-homogeneous polymeric photocatalysts are particularly desirable as they are capable of undertaking photocatalytic reactions in a homogeneous manner, where the polymers are in a fully solvated/swollen state. This results in the photocatalytic moieties being readily accessible by light and substrates. In addition to obtaining an efficient performance, a rapid separation and high recyclability of the catalysts still remains as one of the major challenges. So far, the recycling of pseudo-homogeneous polymeric photocatalysts is typically achieved by either precipitating photocatalytic polymers in organic solvent[30] or extracting the products from the polymer solution,[31] generating waste and increasing the production cost.

In biological systems, conformational changes in response to environmental triggers is utilized to manipulate biochemical activity.[32–35] Mimicking the stimuli-responsive conformational changes in nature, pH-responsiveness could be used to induce a phase transition of the polymeric photocatalyst in aqueous conditions, to allow easy recycling. These pH-triggered phase transitions have been successfully demonstrated by the simple reversible protonation/deprotonation of polyelectrolytes.[36,37] For example, the process of polybase deprotonation promotes the polymer hydrophobicity, leading to a phase separation and recovery of polymer chains from an aqueous solution. However, only few examples of pH-responsive and photoactive polymers[29,38,39] have been demonstrated, although incorporating pH-responsive moieties to polymer structures shows the ability to gain control of the water-compatibility and/or recycling of the materials. Byun et al.[38] reported a CO_2-triggered system, where the wettability of a post-functionalized photocatalytic conjugated linear polymer has been enhanced by the addition of CO_2. Gas exchange provides an orthogonal control of the water-compatibility but, the undefined con-

[*] R. Li, J. Heuer, T. Kuckhoff, K. Landfester, C. T. J. Ferguson
Max Planck Institute for Polymer Research
Ackermannweg 10, 55128 Mainz (Germany)
E-mail: ferguson@mpip-mainz.mpg.de

C. T. J. Ferguson
School of Chemistry, University of Birmingham
Edgbaston, Birmingham, B15 2TT (UK)

© 2023 The Authors. Angewandte Chemie International Edition published by Wiley-VCH GmbH. This is an open access article under the terms of the Creative Commons Attribution License, which permits use, distribution and reproduction in any medium, provided the original work is properly cited.

 © 2023 The Authors. Angewandte Chemie International Edition published by Wiley-VCH GmbH

traction and aggregation of linear polymer chains could lead to an insufficient recovery of the conjugated polymer. Recently, a pH-triggered aggregation of unimolecular micelles, consisting of a Pt-porphyrin photocatalytic center and four poly(dimethylaminoethyl methacrylate) (PDMAEMA) arm chains, has been demonstrated by Zou et al..[39] However, only one reactive center can be incorporated per micelle and the size of the micelle aggregations was still in nm scale (<200 nm) and therefore difficult to recover.

Ideally, the photocatalytic moieties should be solvated/swollen and easily accessible for efficient photocatalysis. Upon the application of an external stimuli they should undergo conformational changes, leading to aggregation and/or precipitation, which facilitates the recovery of the photoactive material. To ensure maximum photocatalytic performance and recovery, this transition should be from the nano to macro scale (visible by eye). A core–shell polymer nanoparticle system that can be homogeneously dispersed in aqueous conditions and stabilized by hydrophilic polymer brushes could be utilized as a polymeric platform for photocatalytic units. Upon elevating the pH, the stabilizing block becomes contracted and nanoparticles aggregate/precipitate. To enable an efficient photocatalytic performance and control, the photocatalytic moieties should be incorporated in the polymer brushes anchored on the surface of the hydrophobic core.

Here, we have produced pH-responsive polymeric core–shell nanoparticles containing photocatalytic active centers distributed within the corona of the nanoparticles. The efficient photocatalytic performance of switchable photocatalytic nanoparticles has been demonstrated by photocatalytic reactions in aqueous medium under visible light irradiation, including photo-reduction of toxic Cr^{VI} inorganic water contamination and various organic transformations (e.g. sulfoxidation, 2-furoic acid oxidation, and Friedel–Crafts alkylation of indole derivative). These nanoparticles undergo stark aggregations upon elevating the pH value of the medium, as the polymer shell turns highly hydrophobic, which facilitates a rapid and easy recovery of the photocatalytic materials (Scheme 1).

pH-responsive polymer photocatalytic nanoparticles were synthesized via reversible addition-fragmentation chain transfer mediated polymerization induced self-assembly (RAFT-PISA) technique,[40] where a pH-responsive photocatalytic macro-chain transfer agent (macroCTA) poly(diisopropylamino ethylmethacrylate-*co*-*N*-(4-(7-phenylbenzo [*c*] [1,2,5] thiadiazol-4-yl)phenyl)methyl methacrylate) (P(DPA-*co*-Ph_2BTMA)) was synthesized prior to its chain extension with hydrophobic benzyl methacrylate (BzMA) monomers. This creates a highly hydrophobic PBzMA core stabilized by protonated P(DPA-*co*-Ph_2BTMA) chains that tether from the surface of the core in acidic buffer conditions (Figure 1a). TEM was applied to confirm the spherical morphology of the nanoparticles (Figure 1b). The hydrodynamic diameter of the photocatalytic material dispersed in acetate buffer (pH 4.0) was determined by DLS, displaying a size distribution centered at around 250 nm (Figure S1).

GPC (Figure S2) has been utilized to examine the molecular weight (Mn = 10.4 kDa) of the polymer photocatalyst. ^{1}H NMR (Figure S3), and FTIR (Figure S4) spectroscopy were used to examine the chemical compositions of photocatalytic polymer nanoparticles. The FTIR spectrum displayed aliphatic backbone ($-CH_2-$ and $-CH_3$) stretch vibration from 2700 to 3100 cm^{-1}. In addition, typical signals at 1720, 1640, and 1170 cm^{-1} are attributed to carbonyl C=O stretching, C=N stretching, and C–O stretching, respectively. The signal at 610–710 cm^{-1} result from the aromatic CH stretch in the PBzMA cores and photocatalytic Ph_2BTMA moieties. The effect of the photocatalytic units on the FTIR spectrum is limited, because only 0.9 mol % of photocatalytic unit has been incorporated. The optical properties of the photocatalytic material was visualized by UV/Vis spectra, displaying a broad absorption peak in the visible

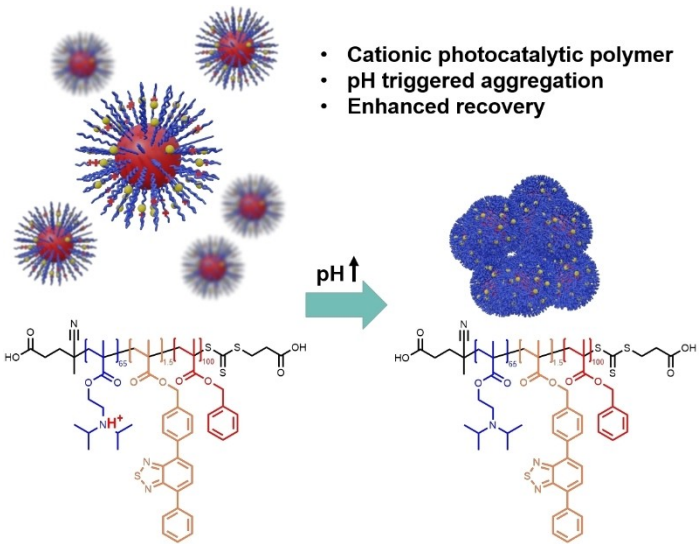

Scheme 1. Illustration of the switchable hydrophilicity of the pH-responsive polymer photocatalyst nanoparticles by adjusting the pH of the solvent.

© 2023 The Authors. Angewandte Chemie International Edition published by Wiley-VCH GmbH

15213773, 2023, 17, Downloaded from https://onlinelibrary.wiley.com/doi/10.1002/anie.202217652 by MPI 355 Polymer Research, Wiley Online Library on [11/04/2023]. See the Terms and Conditions (https://onlinelibrary.wiley.com/terms-and-conditions) on Wiley Online Library for rules of use; OA articles are governed by the applicable Creative Commons License

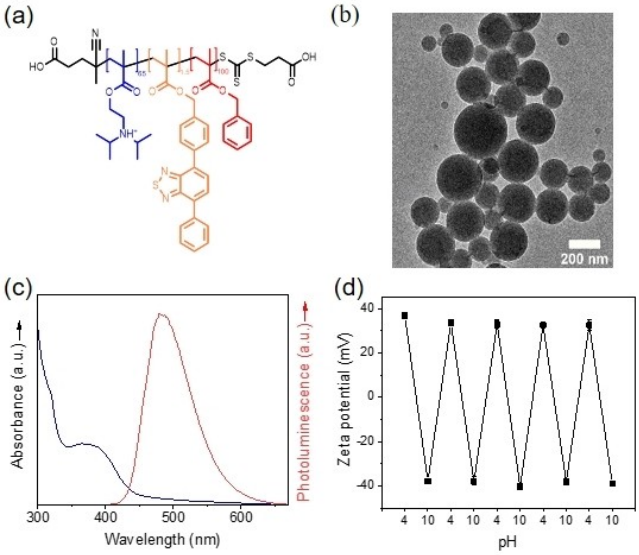

Figure 1. pH-responsive photocatalytic nanoparticles. (a) Molecular structure of designed photocatalytic NP-BT-PDPAH$^+$ nanoparticles. (b) TEM image of the nanoparticle dispersion. (c) UV/Vis absorbance (blue) and emission (red) spectra. (d) Zeta potential of nanoparticle in response to minute change of pH for 5 cycles.

light region up to 600 nm and the peak position at around 390 nm is consistent with literature[28,41] (Figure 1c). The onset reduction potential of the photocatalytic unit diphenylbenzothiadiazole was determined to be −1.34 V vs. SEC (Figure S5) via cyclic voltammetry analysis, which agrees well with value reported previously.[42]

PDPA is a common and inexpensive polymer that can reversibly alter its solubility in water responding to pH changes. The protonation of hydrophobic PDPA chains was simply generated through tuning the water pH below the pKa (pH 6.3, Figure S6) of the tertiary amine. Pristine P(DPA-*co*-Ph$_2$BTMA)-*b*-PBzMA nanoparticles (marked as NP-BT-PDPA) are hydrophobic in neutral water, but upon treating with acid, the tertiary amine end groups of PDPA chains are protonated, leading to a full solvation of PDPA chains and a homogeneous dispersion of nanoparticles (marked as NP-BT-PDPAH$^+$). The proton cations on the tertiary amine can be reversibly removed by adjusting the pH above the pKa and these photocatalytic nanoparticles can be simply recycled by centrifugation or sedimentation (Figure S7). The pH-dependent wettability change of NP-BT-PDPA has been monitored by the UV/Vis transmittance change of nanoparticle dispersion as a function of solvent pH. As shown in Figure S8, the transmittance of the dispersion increased with the elevation of pH, where aggregations have been formed under basic conditions. In addition, the pH-triggered protonation/deprotonation was further investigated by zeta potential (Figure S9). NP-BT-PDPAH$^+$ exhibited a ca. +32 mV of zeta potential at pH 4.0, suggesting a stable positively charged colloid. Upon increasing the solvent pH, zeta potential decreased accordingly. At pH 7.0, a ca. +2 mV of zeta potential was observed, indicating an unstable neutral colloid with a rapid flocculation behavior, agreed well with the pKa value of PDPA (ca. pH 6.3). With further increasing the pH, a negative ca. −36 mV zeta potential was obtained at pH 10.0 possibly due to the interaction between OH$^-$ from buffer solution and the neighboring α-CH groups of tertiary amine acting as Brønsted-Lowry acids. Moreover, the reversibility of protonation/deprotonation process triggered by pH change was also confirmed by zeta potential (Figure 1d), where the zeta potential reversibly switched from ca. +33 mV to −38 mV for 5 cycles by tuning pH between pH 4.0 and pH 10.0.

The switchable hydrophilicity and photocatalytic nature of these newly designed photocatalytic polymer nanoparticles allows the investigation of photocatalysis in acidic aqueous medium. Initially, the photocatalytic activity of NP-BT-PDPAH$^+$ has been demonstrated by photocatalytic reduction of Cr^{VI} under visible light irradiation as a model reaction for heavy-metal-contaminated wastewater treatment. In a typical experimental set-up, an aqueous solution of $K_2Cr_2O_7$ was added to pH-responsive NP-BT-PDPAH$^+$ buffer dispersion (pH 4.0) prior to the irradiation of blue LED light. The reduction of Cr^{VI} was monitored, in triplicate, by UV/Vis spectroscopy. As illustrated in Figure 2a, the positively charged NP-BT-PDPAH$^+$ dispersion produced over 90 % Cr^{VI} reduction after 45 min of light exposure, whereas the control reaction without photocatalyst provided less than 20 % conversion (see Figure S10 for detailed Cr^{VI} reduction kinetic profiles under different conditions). It is worth noting that 55 % of Cr^{VI} reduction has been achieved using NP-BT-PDPAH$^+$ after 2 min of light irradiation without pre-adsorption, which shows an exceptionally high reduction rate compared to the state-of-the-art cationic conjugated polymer photocatalyst[29] and neutral photocatalytic hydrogels.[28]

Furthermore, we have also investigated the Cr^{VI} reduction (Figure 2a) using neutral polymer photocatalytic nanoparticles NP-BT-DHPA (poly(2,3-dihydroxypropyl methacrylate-*co*-*N*-(4-(7-phenylbenzo[*c*][1,2,5]thiadiazol-4-yl)phenyl)methyl methacrylate-*b*-benzylmethacrylate, where only 4 % and 43 % Cr^{VI} reduction was facilitated after 2 and 45 min of light exposure, respectively. The turnover frequency[43] of these neutral NP-BT-DHPA nanoparticles at 5 min was calculated to be 20 times lower than that of cationic NP-BT-PDPAH$^+$ nanoparticles. This strongly suggests that the cationic nature of NP-BT-PDPAH$^+$ has significantly accelerated the conversion rate. Typically, chemical compositions of Cr^{VI} species highly depend on their concentrations and the pH value of the solution.[44,45] Under the present reaction condition at pH 4.0, two predominant species $HCrO_4^-$ and $Cr_2O_7^{2-}$ could present in the form of anions that show high affinities to cationic photocatalytic shell of NP-BT-PDPAH$^+$. Indeed, ion-ion interactions are the strongest non-covalent bond in chemistry.[46–48] This attractive nature of the cationic NP-BT-PDPAH$^+$ to the anionic $HCrO_4^-$ and $Cr_2O_7^{2-}$ substrates drives the substrate diffusion and leads to the enhanced efficiency. Moreover, NP-BT-PDPAH$^+$ nanoparticles were subjected to repeated cycles of Cr^{VI} reduction. No noticeable loss in Cr^{VI} photoreduction efficiency was observed up to 4

© 2023 The Authors. Angewandte Chemie International Edition published by Wiley-VCH GmbH

15213773, 2023, 17, Downloaded from https://onlinelibrary.wiley.com/doi/10.1002/anie.202217652 by MPI 355 Polymer Research, Wiley Online Library on [11/04/2023]. See the Terms and Conditions (https://onlinelibrary.wiley.com/terms-and-conditions) on Wiley Online Library for rules of use; OA articles are governed by the applicable Creative Commons License

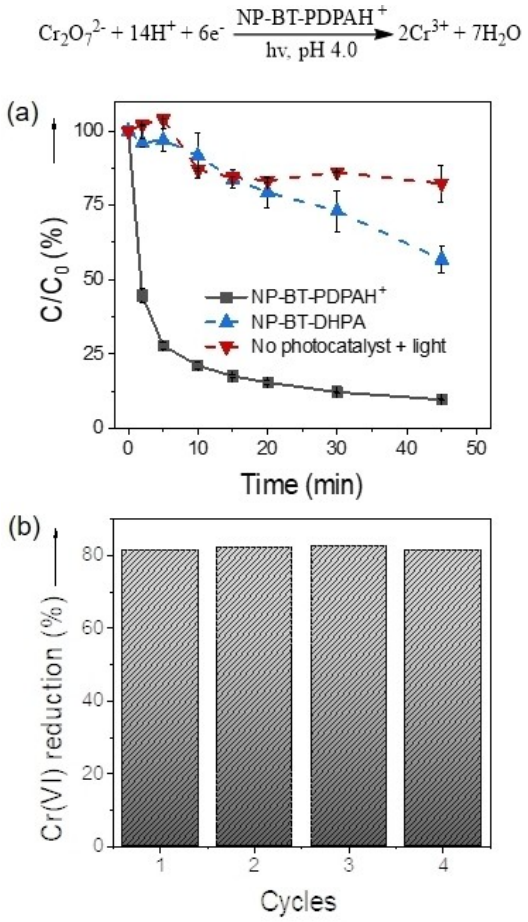

Figure 2. (a) Photocatalytic reduction of Cr^{VI} in NP-BT-DHPA dispersion (pH 4.0), NP-BT-PDPAH$^+$ dispersion (pH 4.0), and without photocatalyst (pH 4.0) under blue LED irradiation (power: 17 mW cm^{-2}, $\lambda = 460$ nm). C_0 is initial concentration of Cr^{VI} under dark condition. C is the concentration of Cr^{VI} with light irradiation after a certain time intervals. (b) Reusability of NP-BT-PDPAH$^+$ for repeated reduction of Cr^{VI}.

cycles (Figure 2b and Figure S10(d), demonstrating an efficient and reusable photocatalytic nanoparticles.

In addition to inorganic heavy metal reduction, the switchable polymer photocatalytic nanoparticles were further applied for various organic transformations. Oxidation reactions, as a fundamental class of organic transformations, have been intensively investigated. Particularly, the sulfoxidation of sulfides is of great importance in many fields, including pharmaceutical industry,[49] wastewater treatment,[28] as well as crude oil desulfurization.[50] Several different photocatalysts[28,51–53] have been utilized for sulfide oxidation, where monoxide product has been produced.

Here, we have utilized the well-dispersed NP-BT-PDPAH$^+$ photocatalyst to induce the oxidation of methyl phenyl sulfide in water. A high yield of 93 % and selectivity of over 99 % monoxide product was observed after 2 h reaction (Table 1 entry 1), which significantly shortens the reaction time compared to the state-of-art photocatalyst (e.g. 18 h, 99 % conversion, 93 % selectivity[51]). Control reactions without photocatalyst or in the dark did not result

Table 1: Photocatalytic sulfoxidation using NP-BT-PDPA in either pH 4.0 or pH 9.0 buffer medium. Reactions were undertaken under blue LED light irradiation (power: 17 mW cm^{-2}, $\lambda = 460$ nm).

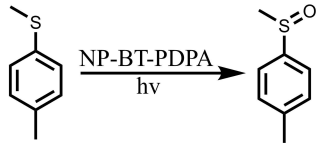

Entry	Catalyst	Light	Time [h]	Yield
1	NP-BT-PDPAH$^+$	+	2	93 %
2	NP-BT-PDPAH$^+$	–	2	0 %
3	–	+	2	0.5 %
4	NP-BT-PDPAH	+	2	36 %
5	Monomer	+	2	34 %

Reaction conditions: Methyl p-tolyl sulfide (50 mM), NP-BT-PDPA (2.5 mg mL^{-1}, 45 μg mL^{-1} photocatalyst), 4 mL buffer solution (Entry 1, 2, 3, and 5: acetate buffer pH 4.0; Entry 4: carbonate-bicarbonate buffer pH 9.0), RT, 2 h, yield determined by GC-MS.

in conversion (Table 1 entry 2&3). Furthermore, the activation/deactivation of photocatalytic moieties as a function of the pH of reaction medium has also been investigated by comparing the sulfoxidation using hydrophobic NP-BT-PDPA dispersion as photocatalyst. A reduced yield (< 36 %) was obtained using NP-BT-PDPA dispersion (Table 1 entry 4) after 2 h of light irradiation. Interestingly, a similar yield (34 %) and reaction kinetics (Figure S11(b)) of sulfoxidation was obtained applying hydrophobic photocatalytic monomers (Table 1 entry 5) at an identical photocatalyst content compared to NP-BT-PDPA nanoparticles. NP-BT-PDPA nanoparticles and photocatalytic monomers are highly hydrophobic, acting as heterogeneous photocatalyst in aqueous solution. Conversely, the greater yield of the sulfoxidation obtained using NP-BT-PDPAH$^+$ dispersion suggests that the pseudo-homogeneous state of photocatalytic sites significantly promotes the reactivity.

Scavenger tests were further performed using sodium azide, potassium iodide, isopropanol, copper chloride, and benzoquinone as $^1O_2$, e^-, $^\bullet OH$, h^+ and $^\bullet O_2^-$ scavenger, respectively. Control reactions in presence of scavengers revealed that $^1O_2$, h^+ and $^\bullet O_2^-$ are crucial for the sulfoxidation (Figure S12, Table S1). Furthermore, NP-BT-PDPAH$^+$ were subjected to repeated cycles of sulfide oxidation through acidic/basic solvent switching, therefore, nanoparticle precipitation and redispersion. No perceptible loss in sulfide oxidation efficiency was observed after 4 cycles, despite of a slight loss of nanoparticles after 2nd run of the recycling experiments (Figure S13).

NP-BT-PDPAH$^+$ is capable of efficiently generating $^1O_2$ (Figure S14), which has been widely used to drive oxidation reactions. As displayed in Table 2 (Entry 1), a well-known $^1O_2$ trap, 2-furoic acid was effectively oxidized to 5-hydroxy-2(5H)-furanone in the presence of oxygen with a yield of > 99 % after 20 h. Control reactions (Table S2) in the closed air condition, in dark, and without photocatalyst produced 30 %, < 1 %, and < 1% of yield, respectively, indicating oxygen and photocatalyst with light irradiation are required to facilitate sufficient $^1O_2$ generation. NP-BT-PDPAH$^+$

© 2023 The Authors. Angewandte Chemie International Edition published by Wiley-VCH GmbH

15213773, 2023, 17, Downloaded from https://onlinelibrary.wiley.com/doi/10.1002/anie.202217652 by MPI 355 Polymer Research, Wiley Online Library on [11/04/2023]. See the Terms and Conditions (https://onlinelibrary.wiley.com/terms-and-conditions) on Wiley Online Library for rules of use; OA articles are governed by the applicable Creative Commons License

Table 2: Photocatalytic conversion of organic molecules using NP-BT-PDPA-H$^+$ in pH 4.0 buffer media. Reactions were undertaken under blue LED light irradiation (power: 17 mW cm^{-2}, $\lambda = 460$ nm).

Entry	Reaction	Time	Conv.	Yield
(1)[a] Oxidation reaction	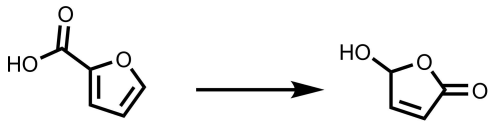	20 h	>99%	>99%
(2)[b] Redox reaction	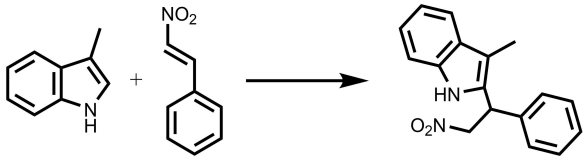	14 h	80%	70%

Reaction conditions: [a] 2-Furoic acid (0.15 M), NP-BT-PDPAH$^+$ (2.5 mg mL^{-1}, 45 μg mL^{-1} photocatalyst), acetate buffer pH 4.0 (4 mL), RT, 20 h. Conversion determined by NMR spectroscopy. [b] 3-methyl indole (19 mM), β-nirtostyrene (20 mM), NP-BT-PDPAH$^+$ (2.5 mg mL^{-1}, 45 μg mL^{-1} photocatalyst), acetate buffer pH 4.0 (10 mL), RT, 14 h. Conversion and yield detected by GC-MS.

nanoparticles have facilitated over 95% conversion of 2-furoic acid up to five 24 h-cycles without losing the conversion efficiency (Figure S15). Moreover, extremely high material recovery was maintained throughout the recycling tests (Figure S16), suggesting the high recyclability and stability of NP-BT-PDPAH$^+$ photocatalyst. It is worth noting that consideration to substrate choice is required for the proper recycling of these photocatalytic nanoparticles.

The promising performance of NP-BT-PDPAH$^+$ in the photocatalytic reductive and oxidative transformations has encouraged us to examine its potential in performing redox reactions. Indole has been widely used as an important building block for the production of biologically active compounds.[54,55] The N-1, C-2 to C-6, or C-7 positions of indole can be substituted to produce versatile indole derivatives, demonstrating a diverse scaffold for drug design.[56–59] Recently, a new strategy for the photocatalytic production of Friedel–Crafts alkylation at C-3 position of indoles through the reaction of indoles and nitroalkenes has been reported, where water has been used as a green solvent.[60] However, relatively high temperature (60 °C) was required to accelerate these reactions. Therefore, we have investigated the radical-mediated Friedel–Crafts alkylation at room temperature to further verify the versatility of NP-BT-PDPAH$^+$. Surprisingly, our attempts showed that the coupling at the C-3 position of indole derivatives proceeded under blue light irradiation without photocatalyst at ambient temperature. The high yield in the absence of NP-BT-PDPAH$^+$ may proceed through a free radical pathway proposed by a previous investigation, where 1,3 H shift of indole was activated by blue light irradiation followed by the generation of an indole radical to initiate the coupling reaction.[61] However, no products with substituent at the C-2 position of indole molecule have been reported in previous scope of studies, possibly because of the low reactivity of the C-2 position of indole.[60–62]

Indole derivatives substituted at the indole C-2 and C-3 positions have been widely applied as target-based anti-cancer inhibitors and some of these therapeutics have been approved by FDA.[59] In particular, indole-based tubulin inhibitors are of great importance that inhibit the polymerization of tubulin, thereafter suppress mitosis and induce appotosis of cancer cells.[57–59] In our investigation, 3-methyl indole has been selected as a simple C-3 substituted model indole derivative, where additionally the aforementioned 1,3 H shift process initiated by light may be suppressed. Here, the alkylation of 3-methyl indole and β-nitrostyrene proceeded to afford a 70% yield by adding NP-BT-PDPAH$^+$ (Table 2 entry 2), where the control reaction proceeded with 19% yield without photocatalyst. Without light illumination, no coupling product was formed after 20 h. Although oxidation byproducts of 3-methyl indole and direct [2+2] addition of β-nitrostyrene were observed, photoredox-induced alkylation was still dominant. A possible mechanism[60] of this C–C coupling was illustrated in Figure S17. Upon visible-light irradiation, photocatalyst was excited and 3-methyl indole gave an electron to the highest occupied molecular orbital (HOMO) of the photocatalyst, generating a radical. The resultant 3-methylindole radical reacted with the double bond of β-nitrostyrene to produce a radical intermediate. This intermediate was further reduced by the photo-promoted electron in the lowest unoccupied molecular orbital (LUMO) of the photocatalyst giving a negatively charged intermediate. After protonation, the final coupled product was obtained.

In summary, we have demonstrated novel pH-responsive polymer photocatalytic nanoparticles, containing diisopropylamino moieties as pH-sensitive functional groups and a small portion of photocatalytic moieties. pH-triggered hydrophobicity change of the stabilizing PDPA block enables controllable photocatalysis in aqueous environment. In acidic conditions (pH 4.0) below the pKa of PDPA block, the photocatalytic moieties are in a pseudo-homogeneous state facilitating effective catalytic activity towards both inorganic and organic transformations, including photo-reduction of Cr^{VI} and photo-redox Friedel–Crafts alkylation of indole derivative. These reactions exhibited a nanoparticle concentration dependence. Moreover, the charged PDPAH$^+$ block is capable of not only enhancing the dispersibility of the nanoparticles, but also accelerating photocatalytic reactions of anionic substrates owing to charge attraction interactions. Furthermore, by simply

© 2023 The Authors. Angewandte Chemie International Edition published by Wiley-VCH GmbH

15213773, 2023, 17, Downloaded from https://onlinelibrary.wiley.com/doi/10.1002/anie.202217652 by MPI 355 Polymer Research, Wiley Online Library on [11/04/2023]. See the Terms and Conditions (https://onlinelibrary.wiley.com/terms-and-conditions) on Wiley Online Library for rules of use; OA articles are governed by the applicable Creative Commons License

tuning the pH above the pKa of the stabilizing PDPA block, photocatalytic nanoparticles with unaltered morphology and composition have been recycled, allowing a sustainable performance. This strategy produces highly effective polymeric photocatalytic nanoparticles with great photocatalytic performance, switchability, and recyclability.

Acknowledgements

The authors acknowledge the Max Planck Graduate Center (MPGC) for funding. Open Access funding enabled and organized by Projekt DEAL.

Conflict of Interest

The authors declare no conflict of interest.

Data Availability Statement

The data that support the findings of this study are available from the corresponding author upon reasonable request.

Keywords: Enhanced Recyclability · Photocatalysis · pH-Responsive Photocatalytic Nanoparticles

[1] C. Lu, P. Zhang, S. Jiang, X. Wu, S. Song, M. Zhu, Z. Lou, Z. Li, F. Liu, Y. Liu, Y. Wang, Z. Le, *Appl. Catal. B* **2017**, *200*, 378–385.
[2] S. Ghosh, N. A. Kouamé, L. Ramos, S. Remita, A. Dazzi, A. Deniset-Besseau, P. Beaunier, F. Goubard, P.-H. Aubert, H. Remita, *Nat. Mater.* **2015**, *14*, 505–511.
[3] W. Deng, H. Zhao, F. Pan, X. Feng, B. Jung, A. Abdel-Wahab, B. Batchelor, Y. Li, *Environ. Sci. Technol.* **2017**, *51*, 13372–13379.
[4] O. Fawzi Suleiman Khasawneh, P. Palaniandy, *Environ. Technol. Innovation* **2021**, *21*, 101230.
[5] J. Geng, C. Sun, J. Liu, L.-D. Liao, Y. Yuan, N. Thakor, J. Wang, B. Liu, *Small* **2015**, *11*, 1603–1610.
[6] S. Kwiatkowski, B. Knap, D. Przystupski, J. Saczko, E. Kędzierska, K. Knap-Czop, J. Kotlińska, O. Michel, K. Kotowski, J. Kulbacka, *Biomed. Pharmacother.* **2018**, *106*, 1098–1107.
[7] J. H. Correia, J. A. Rodrigues, S. Pimenta, T. Dong, Z. Yang, *Pharmaceutica* **2021**, *13*, 1332.
[8] J. C. S. Simões, S. Sarpaki, P. Papadimitroulas, B. Therrien, G. Loudos, *J. Med. Chem.* **2020**, *63*, 14119–14150.
[9] V. S. Vyas, F. Haase, L. Stegbauer, G. Savasci, F. Podjaski, C. Ochsenfeld, B. V. Lotsch, *Nat. Commun.* **2015**, *6*, 8508.
[10] S. Cao, L. Piao, X. Chen, *Trends Chem.* **2020**, *2*, 57–70.
[11] W. Zhao, Z. Chen, X. Yang, X. Qian, C. Liu, D. Zhou, T. Sun, M. Zhang, G. Wei, P. D. Dissanayake, Y. S. Ok, *Renewable Sustainable Energy Rev.* **2020**, *132*, 110040.
[12] J. Kosco, M. Bidwell, H. Cha, T. Martin, C. T. Howells, M. Sachs, D. H. Anjum, S. Gonzalez Lopez, L. Zou, A. Wadsworth, W. Zhang, L. Zhang, J. Tellam, R. Sougrat, F. Laquai, D. M. DeLongchamp, J. R. Durrant, I. McCulloch, *Nat. Mater.* **2020**, *19*, 559–565.
[13] S. Liu, W. Pan, S. Wu, X. Bu, S. Xin, J. Yu, H. Xu, X. Yang, *Green Chem.* **2019**, *21*, 2905–2910.
[14] H.-P. Liang, Q. Chen, B.-H. Han, *ACS Catal.* **2018**, *8*, 5313–5322.
[15] G. H. Lovett, S. Chen, X.-S. Xue, K. N. Houk, D. W. C. MacMillan, *J. Am. Chem. Soc.* **2019**, *141*, 20031–20036.
[16] L. Tian, N. A. Till, B. Kudisch, D. W. C. MacMillan, G. D. Scholes, *J. Am. Chem. Soc.* **2020**, *142*, 4555–4559.
[17] J. Kim, B. X. Li, R. Y.-C. Huang, J. X. Qiao, W. R. Ewing, D. W. C. MacMillan, *J. Am. Chem. Soc.* **2020**, *142*, 21260–21266.
[18] A. Mills, C. O'Rourke, *Catal. Today* **2014**, *230*, 256–264.
[19] C. Ayed, L. C. da Silva, D. Wang, K. A. I. Zhang, *J. Mater. Chem. A* **2018**, *6*, 22145–22151.
[20] D. A. Nagib, D. W. C. MacMillan, *Nature* **2011**, *480*, 224–228.
[21] R. Pawlowski, F. Stanek, M. Stodulski, *Molecules* **2019**, *24*, 1533.
[22] Z. Li, W. Zhang, Q. Zhao, H. Gu, Y. Li, G. Zhang, F. Zhang, X. Fan, *ACS Sustainable Chem. Eng.* **2015**, *3*, 468–474.
[23] C. K. Prier, D. A. Rankic, D. W. C. MacMillan, *Chem. Rev.* **2013**, *113*, 5322–5363.
[24] N. A. Romero, D. A. Nicewicz, *Chem. Rev.* **2016**, *116*, 10075–10166.
[25] L. Wang, W. Huang, R. Li, D. Gehrig, P. W. M. Blom, K. Landfester, K. A. I. Zhang, *Angew. Chem. Int. Ed.* **2016**, *55*, 9783–9787; *Angew. Chem.* **2016**, *128*, 9935–9940.
[26] R. Radjagobalou, J.-F. Blanco, L. Petrizza, M. Le Bechec, O. Dechy-Cabaret, S. Lacombe, M. Save, K. Loubiere, *ACS Sustainable Chem. Eng.* **2020**, *8*, 18568–18576.
[27] T. Banerjee, F. Podjaski, J. Kröger, B. P. Biswal, B. V. Lotsch, *Nat. Rev. Mater.* **2021**, *6*, 168–190.
[28] T. Kuckhoff, K. Landfester, K. A. I. Zhang, C. T. J. Ferguson, *Chem. Mater.* **2021**, *33*, 9131–9138.
[29] S. Ghasimi, K. Landfester, K. A. I. Zhang, *ChemCatChem* **2016**, *8*, 694–698.
[30] J. J. Lessard, G. M. Scheutz, A. B. Korpusik, R. A. Olson, C. A. Figg, B. S. Sumerlin, *Polym. Chem.* **2021**, *12*, 2205–2209.
[31] M. Bu, C. Cai, F. Gallou, B. H. Lipshutz, *Green Chem.* **2018**, *20*, 1233–1237.
[32] R. Wang, X. Qi, P. Schmiege, E. Coutavas, X. Li, *Sci. Adv.* **2020**, *6*, eaaz1466.
[33] C. Narayanan, D. N. Bernard, K. Bafna, D. Gagné, P. K. Agarwal, N. Doucet, *Front. Mol. Biosci.* **2018**, *5*, 54.
[34] B. Moree, K. Connell, R. B. Mortensen, C. T. Liu, S. J. Benkovic, J. Salafsky, *Biophys. J.* **2015**, *109*, 806–815.
[35] J.-H. Ha, S. N. Loh, *Chem. Eur. J.* **2012**, *18*, 7984–7999.
[36] S. Biswas, E. Mani, A. Mondal, A. Tiwari, S. Roy, *Soft Matter* **2016**, *12*, 1989–1997.
[37] J. D. Willott, W. M. Nielen, W. M. de Vos, *ACS Appl. Polym. Mater.* **2020**, *2*, 659–667.
[38] J. Byun, W. Huang, D. Wang, R. Li, K. A. I. Zhang, *Angew. Chem. Int. Ed.* **2018**, *57*, 2967–2971; *Angew. Chem.* **2018**, *130*, 3019–3023.
[39] Q. Zuo, K. Feng, J. Zhong, Y. Mai, Y. Zhou, *CCS Chem.* **2021**, *3*, 1963–1971.
[40] F. D'Agosto, J. Rieger, M. Lansalot, *Angew. Chem. Int. Ed.* **2020**, *59*, 8368–8392; *Angew. Chem.* **2020**, *132*, 8444–8470.
[41] C. T. J. Ferguson, N. Huber, K. Landfester, K. A. I. Zhang, *Angew. Chem. Int. Ed.* **2019**, *58*, 10567–10571; *Angew. Chem.* **2019**, *131*, 10677–10681.
[42] N. Huber, R. Li, C. T. J. Ferguson, D. W. Gehrig, C. Ramanan, P. W. M. Blom, K. Landfester, K. A. I. Zhang, *Catal. Sci. Technol.* **2020**, *10*, 2092–2099.
[43] S. Kozuch, J. M. L. Martin, *ACS Catal.* **2012**, *2*, 2787–2794.
[44] P. C. Bandara, J. Peña-Bahamonde, D. F. Rodrigues, *Sci. Rep.* **2020**, *10*, 9237.
[45] Y. Chen, D. An, S. Sun, J. Gao, L. Qian, *Materials* **2018**, *11*, 269.

© 2023 The Authors. Angewandte Chemie International Edition published by Wiley-VCH GmbH

15213773, 2023, 17, Downloaded from https://onlinelibrary.wiley.com/doi/10.1002/anie.202217652 by MPI 355 Polymer Research, Wiley Online Library on [11/04/2023]. See the Terms and Conditions (https://onlinelibrary.wiley.com/terms-and-conditions) on Wiley Online Library for rules of use; OA articles are governed by the applicable Creative Commons License

[46] J. R. Stutzman, C. A. Luongo, S. A. McLuckey, *J. Mass Spectrom.* **2012**, *47*, 669–675.
[47] P. Kollman, in *New Comprehensive Biochemistry* (Ed.: M. I. Page), Elsevier, Amsterdam, **1984**, pp. 55–71.
[48] P. Kumar, S. Banerjee, A. Radha, T. Firdoos, S. Chandra Sahoo, S. K. Pandey, *New J. Chem.* **2021**, *45*, 2249–2263.
[49] S. Caron, R. W. Dugger, S. G. Ruggeri, J. A. Ragan, D. H. B. Ripin, *Chem. Rev.* **2006**, *106*, 2943–2989.
[50] S. Otsuki, T. Nonaka, N. Takashima, W. Qian, A. Ishihara, T. Imai, T. Kabe, *Energy Fuels* **2000**, *14*, 1232–1239.
[51] C. T. J. Ferguson, N. Huber, T. Kuckhoff, K. A. I. Zhang, K. Landfester, *J. Mater. Chem. A* **2020**, *8*, 1072–1076.
[52] Y. Huang, Z. Xin, W. Yao, Q. Hu, Z. Li, L. Xiao, B. Yang, J. Zhang, *Chem. Commun.* **2018**, *54*, 13587–13590.
[53] C. Herrero, A. Quaranta, R. Ricoux, A. Trehoux, A. Mahammed, Z. Gross, F. Banse, J.-P. Mahy, *Dalton Trans.* **2016**, *45*, 706–710.
[54] M. M. Heravi, Z. Amiri, K. Kafshdarzadeh, V. Zadsirjan, *RSC Adv.* **2021**, *11*, 33540–33612.
[55] T. C. Barden, in *Heterocyclic Scaffolds II: Reactions and Applications of Indoles* (Ed.: G. W. Gribble), Springer, Berlin, Heidelberg, **2010**, pp. 31–46.
[56] A. Dorababu, *RSC Med. Chem.* **2020**, *11*, 1335–1353.
[57] F. Naaz, K. Neha, M. R. Haider, S. Shafi, *Future Med. Chem.* **2021**, *13*, 1795–1828.
[58] Y. Hong, Y.-Y. Zhu, Q. He, S.-X. Gu, *Bioorg. Med. Chem.* **2022**, *55*, 116597.
[59] S. Tang, Z. Zhou, Z. Jiang, W. Zhu, D. Qiao, *Molecules* **2022**, *27*, 1587.
[60] Z.-Y. Yu, J.-N. Zhao, F. Yang, X.-F. Tang, Y.-F. Wu, C.-F. Ma, B. Song, L. Yun, Q.-W. Meng, *RSC Adv.* **2020**, *10*, 4825–4831.
[61] S. Yadav, M. Srivastava, P. Rai, B. P. Tripathi, A. Mishra, J. Singh, J. Singh, *New J. Chem.* **2016**, *40*, 9694–9701.
[62] R. P. Herrera, V. Sgarzani, L. Bernardi, A. Ricci, *Angew. Chem. Int. Ed.* **2005**, *44*, 6576–6579; *Angew. Chem.* **2005**, *117*, 6734–6737.

Manuscript received: November 30, 2022
Accepted manuscript online: February 7, 2023
Version of record online: March 16, 2023

© 2023 The Authors. Angewandte Chemie International Edition published by Wiley-VCH GmbH

15213773, 2023, 17, Downloaded from https://onlinelibrary.wiley.com/doi/10.1002/anie.202217652 by MPI 355 Polymer Research, Wiley Online Library on [11/04/2023]. See the Terms and Conditions (https://onlinelibrary.wiley.com/terms-and-conditions) on Wiley Online Library for rules of use; OA articles are governed by the applicable Creative Commons License